Heliyon 10 (2024) e32396

Contents lists available at ScienceDirect

Heliyon

journal homepage: www.cell.com/heliyon

Research article

Characterization of groundwater salinity by hydrogeochemical and multivariate statistical analysis in the coastal aquifer of Nagapattinam district, Southern India

Ratnakar Dhakate

CSIR-National Geophysical Research Institute, (Council of Scientific & Industrial Research), Uppal Road, Hyderabad, 500007, India

ARTICLE INFO

Keywords:
Factor analysis (FA)
Cluster analysis (CA)
Seawater intrusion and Total Dissolved Solids (TDS)

ABSTRACT

The impact of seawater intrusion from coast to inland terrain in the Cauvery River Basin (CRB) and Uppanar River Basin (URB) was evaluated based on major ion groundwater chemistry. TDS ranges from 229 to 2260 mg/l, and 408 to 3732 mg/l; Na^+ range from 67 to 560 mg/l, and 74 to 1600 mg/l, and Cl^- range from 120 to 906 mg/l, and 110 to 3260 mg/l for CRB and URB respectively. Piper Diagram, Hydrochemical Facies Evolution Diagram (HFE-D), rock-water interaction (Gibbs Plots), various bivariate plots viz., TDS vs. Cl^-; Na^+ vs. Cl^-; Ca^{2+} vs. Cl^-; Ca^{2+} vs. SO_4^{2-}; TH vs. TDS and Principal Component Analysis (PCA) (Cluster and Factor analysis) were used to identify the seawater intrusion from coast to inland aquifers and to understand hydrogeochemical characterization and salinization processes. Piper diagram shows that most of the samples are Na^+-Cl^- type, HFE-D diagram also shows that most of the samples were saline intrusion type and mixing behavior, while TH *vs.* TDS plot shows hard fresh to hard brackish type from both the basins. PCA results clearly show the three factors, explaining 84.02 % and 76.67 % variance in URB and CRB. Factor-1 records 53.03 % alteration, with a strong confidence loading of TDS, Na^+, Cl^-, Ca^{2+}, K^+, SO_4^2, Total Alkalinity (TA), and Total Hardness (TH) in URB indicating saline nature. A total variance of 46.23 % in CBR is more positively loaded with TH, Mg^{2+}, Ca^{2+}, and SO_4^{2-} indicating rock-water interaction. Cluster analyses of these parameters illustrate the cluster distribution in CRB and URB. In URB, TDS, Na^+, and Cl^- ions make a cluster with a linkage distance of 5000 m, whereas in CRB, the TDS, Na^+, Cl^-, and TA ions make a cluster with a linkage distance of 2800 m. The factor and cluster analysis fetched out an effect of intensive use of fertilizers, aquaculture activities, and excessive groundwater exploitation. This technique gave the relationship between various chemical parameters in groundwater. Factor and cluster analysis have proven highly effective in groundwater quality studies. The study concluded that the study area has the threat of saline water intrusion in shallow aquifers with continuous influences of seawater mixing.

1. Introduction

The coastal regions of India are the most densely populated having a population mass of about 80 persons or even more per sq. km [1,2]. The coastal aquifers were always under tremendous stress for fresh groundwater exploitation to satisfy the primary demands of fresh water for various purposes [3]. The unwarranted exploitation of fresh water from coastal regions will disturb the hydrodynamic balance between freshwater and seawater and become the cause driving seawater into the freshwater [4]. Seawater intrusion extent and fluctuations broadly vary from region to region. Several studies by different researchers have been investigated in coastal regions

https://doi.org/10.1016/j.heliyon.2024.e32396
Received 2 January 2024; Received in revised form 3 June 2024; Accepted 3 June 2024
Available online 4 June 2024

around the globe to recognize seawater intrusion problems using different indicators [3,5–13].

To understand the seawater intrusion processes groundwater hydrochemistry plays an important role. Various ratios and plots suggested by several researchers earlier were used to understand the natural and anthropogenic activities for evaluating the hydrochemical processes taking place in the aquifer regime for deteriorating the fresh aquifer by saline water intrusion. The fresh and saline water zones in coastal areas were also demarcated and resolved by electrical resistivity and ground penetrating radar methods to locate the freshwater zones in saline-affected areas [14–19].

Principal Component Analysis (Factor and Cluster) has been widely used for data reduction and drawing an appropriate and thoughtful decision of data. These tools (Factor and Cluster) have been used by several researchers to draw meaningful and unbiased conclusions about water quality data sets [20–26]. Using statistical techniques, the time-based and periodic disparity of river water quality analyses caused by natural or anthropogenic processes has been evaluated [27]. Principal Component Analysis (PCA) which includes Factor and Cluster analysis was a very useful practical method to decrease large data sets of inter-related variables and their dimensionality. This decrease of data sets was performed by transmuting the old data sets into a new meaningful and understandable data set of known variables as principal components (PCs) which were organized in decreasing order of importance variable. PCs are the direct grouping of the original variables and the eigenvalues [28]. The method used for the interpretation of the physical and chemical composition of groundwater data a graphical way of presentation, such as a Piper diagram and statistical analysis [29–31]. However, these presentation results may be misleading interpretations and conclusions [32]. To overcome this problem, multivariate statistical analysis with other combinations of various plots can be used, which can be an unbiased method of representing the association between samples or variables to highlight information in a much better way [33–35]. Recently, many researchers have accepted factor and cluster analysis techniques to resolve and assess groundwater quality-related problems and intrusion of fresh-saline water [20,32,36,37].

The main determination and objective of the study are to illustrate the problem that has been incurred by agriculture, aquaculture, and backwater flow in the Cauvery River Basin (CRB) and Uppanar River Basin (URB) for a longer time, thus making groundwater fresh-saline mixture from the coast towards the inland. The groundwater has been severely degraded by salinization and this salinization of the groundwater may have been caused by agricultural, aquaculture activities, or heavy pumping. The URB has a very low elevation compared to the CRB. The hydrochemical differentiation of salinization processes in coastal areas is very complex because there is a considerable amount of hydrogeochemical variability due to the superposition of different processes, such as seawater intrusion and pollution phenomena. This study demonstrates the effectiveness of Factor and Cluster Analysis as a tool for the assessment of the scope of ionic concentration and factors affecting groundwater quality in the coastal aquifer system of both URB and CRB.

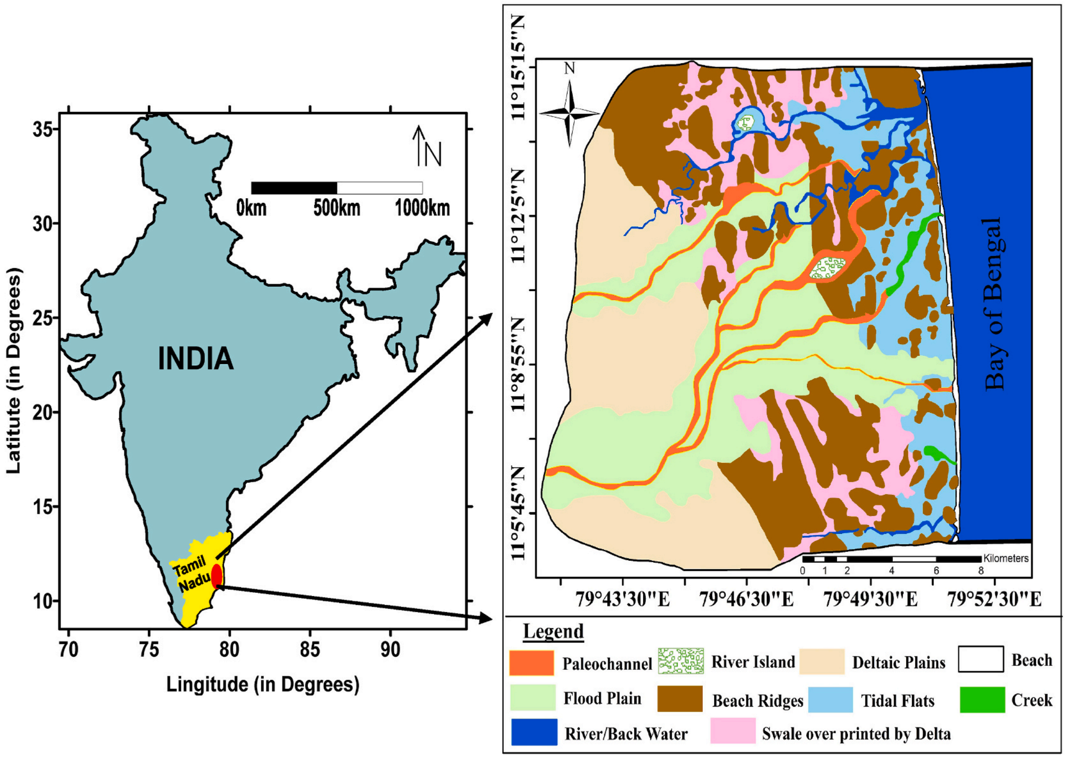

Fig. 1. Geomorphologic units of Cauvery River Basin and Uppanar River Basin, Nagapattinam, Tamil Nadu, India.

2. Study area

The study area belongs to longitude 79^0 42’ 00″ to 79^0 51’ 30″ E and latitudes 11^0 05’ 00″ to 11^0 15’ 30” N with an area of 316.2 km^2 (Fig. 1). The URB with an area of 168.8 km^2 and CRB with an area of 147.4 km^2 are located in Nagapattinam District, Tamil Nadu, India. The area has a flat topography with few beach ridges. In CRB the relief varies from 0 to 17.3 m above mean sea level (AMSL) and the inundation of backwater within 5 km from the coastline with topography was <3 m (AMSL). The elevation of the URB varies from 0 to 14.33 m (AMSL) and is as low as <3 m (AMSL). The backwater in URB proceeds inland up to a distance of 20 km distance. The average annual rainfall varies from 1200 to 1500 mm/year contributed by the North-East monsoon during October–December. Economically this area depends on agriculture, prawn cultivation, and brick industries.

3. Geology, geomorphology and hydrology

The geology of the area is identified as sediments deposits of quaternary age from the River Cauvery and its tributaries (Cauvery Formation), deltaic fluviomarine plain (Nagapattinam Formation), and marine coastal plain (East Coast formation) deposits [38]. Few paleo channels with an admixture of silt, sand, clay, and gravel were noticed. The deltaic plain includes paleo tidal flats with sand, clay, silt, and ridges of grey-brown sands. Tidal flats, deposits of sand, clay, and tidal clays form the marine coastal plains. Geomorphically the study area is divided into three major geomorphological units viz., fluvial unit, fluviomarine unit, and marine unit (Fig. 1). Generally, groundwater occurs in unconfined and semi-confined nature and it is characterized by sands, gravel, sandy clays, and variegated clays and its thickness varied from 10 to 35 m [39]. The groundwater was mined from shallow tube wells and dug-cum-borewells. Freshwater pockets were found only in dunes and beach ridges.

4. Methods and materials

4.1. Sampling and analytical method

At 37 locations groundwater samples were collected during the post-monsoon season of 2003 to assess the major ion chemistry. Groundwater samples at 20 locations were collected from CRB and 17 locations from URB from shallow tube wells and dug-cum borewells and analyzed for major ions chemistry (Fig. 2). A clean plastic container of 1-L volume was used for sample collection. The container was rinsed thoroughly with the sample water before collecting the samples, numbered sequentially, and brought to the laboratory. Physical parameters for example pH and Electrical Conductivity (EC) were measured with the help of portable EC and pH meter of NACH HQ 40 d m and chemical parameters such as major ions, Cl^-, HCO_3^-, F^-, SO_4^{2-}, NO_3^-, Na^+, Ca^{2+}, K^+, Mg^{2+}, were analyzed by following standard methods [40]. Flame photometry was used to analyze the amount of Na^+, and K^+ in the given water samples by using the CL-345 flame photometer of ELICO. A UV-V spectrometer was used to estimate the amount of NO_3^- with two different wavelengths 220 nm and 275 nm. By using a UV-V spectrophotometer fluoride concentration was analyzed at 570 nm wavelength using the colorimetric method. SO_4^{2-} was analyzed by using the NEPHELO Turbidity meter at 425 nm wavelength. Cl^-, HCO_3^-, Ca^{2+}, and TH ions were analyzed by using the standard volumetric titration method. Water must be electrically neutral; the sum of cations should be equal to the sum of the anion. Total Dissolved Solids (TDS) were calculated from EC with a multiplication factor of 0.64. The accuracy of the results of all parameters was evaluated by using a charge balance error (CBE) which must be less than ±5 % and was compared with the water quality standards [41]. The statistical summary of analysis samples is given in (Table 1).

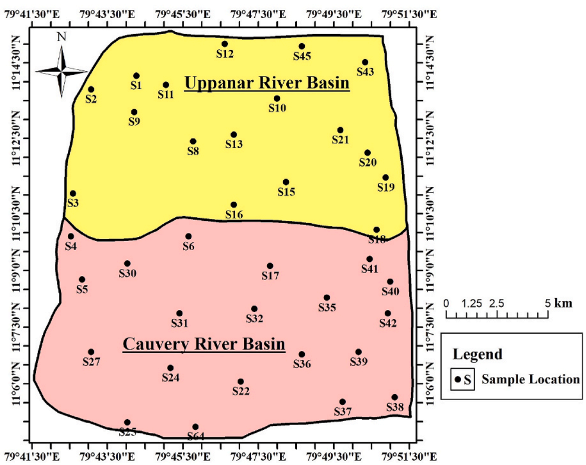

Fig. 2. Sample location in the Cauvery and Uppanar River Basin.

Table 1
Physico-chemical analyses of groundwater samples of Cauvery River Basin and Uppanar River Basin.

Parameters	Cauvery River Basin (CRB) (n = 20)				Uppanar River Basin (URB) (n = 17)			
	Min	Max	Ave	SD	Min	Max	Ave	SD
pH	7.30	8.90	8.30	0.50	7.20	8.70	7.90	0.40
EC (μS/cm)	358	2260	1182.30	566	637	5830	2281.50	1500.30
TDS (mg/l)	229	1446	748.30	362.39	408	3732	1388.47	948.30
TA (mg/l)	220	520	347.50	91.64	160	680	354.12	124.45
TH (mg/l)	48	480	201	106.02	104	560	354.12	130.71
Ca^{2+} (mg/l)	12	92	54	23.56	32	356	308.94	130.71
Mg^{2+} (mg/l)	36	400	147	87.83	68	340	197.65	70.31
Na^{+} (mg/l)	67	560	282.75	162.99	74	1600	508.59	427.58
K^{+} (mg/l)	42	280	128.75	51.08	63	502	216.18	102.19
NO_3^- (mg/l)	1	158.50	23.55	36.22	1	328.80	45.39	79.84
Cl^- (mg/l)	120	906	381.27	225.03	110	3260	724.71	798.89
SO_4^{2-} (mg/l)	8.80	260	75.84	68.04	20	406.30	181.12	122.65
F^- (mg/l)	0	1.20	0.33	0.27	0.10	0.70	0.32	0.22
HCO_3^- (mg/l)	268.40	634.40	423.95	111.81	195.20	829.60	432.02	151.83

NOTE: TDS = Total Dissolved Solid; TA = Total Alkalinity; TH = Total Hardness; Min = Minimum; Max = Maximum; Avg = Average and SD= Standard Deviation.

4.2. *Statistical method*

To evaluate the Factor and Cluster analysis SPSS 23 software was used. Cluster analysis was achieved for original data by using Ward's and Euclidean distance methods. The eigenvalues were figured out for all the axes, and with a minimum eigenvalue of >1, factor extraction has been done [33]. The factor loading matrix is rotated on a simple orthogonal structure, depending on the varimax rotation, which makes it possible to maximize the variance of the variable factor load with the generation of a new matrix describing each factor and allows better ease of interpretation (Table 2). The explained variance was computed for the respective variables with a respective factor with a quadrant of appropriate factor load. The residual variance obtained for the respective variable was determined by adding the variance.

5. Result and discussions

Groundwater samples at 37 sampling sites were analyzed for 11 constituents including the major anions and cations as shown in (Table 1). The chemical analysis data of the groundwater sampled were analyzed to understand the background factors. The 11 constitutes are treated as 11 observable quantity variables with the covariance matrix composed for the multivariate analysis.

5.1. *Physical-chemical compositions*

A statistical summary of the physical and chemical compositions of the groundwater samples is presented in (Table 1). pH values ranged from 7.30 to 8.90 and 7.20 to 8.70 for CRB and URB. The Electrical Conductivity (EC) value of groundwater ranges from 358 to 2260 μS/cm, and 637 to 5830 μS/cm, and TDS value ranges from 229 to 1446 mg/l and 408 to 3732 mg/l for CRB and URB, and shows a rapid elevating trend toward the coastline (Table 1 and Fig. 3). Most of the chemical parameters also have a similar trend to that of

Table 2
Principal component (PC) analysis of Groundwater chemistry data for Cauvery River Basin and Uppanar River Basin.

Parameters	Cauvery River Basin			Uppanar River Basin		
	PC-1	PC-2	PC-3	PC-1	PC-2	PC-3
TDS	0.44	0.86	0.06	0.93	−0.15	0.17
TA	−0.13	0.81	0.00	−0.11	−0.95	0.15
TH	0.97	0.17	0.01	0.81	0.11	0.52
Ca^{2+}	0.81	0.11	0.38	0.89	0.31	0.12
Mg^{2+}	0.95	0.17	−0.07	0.39	−0.18	0.82
Na^{+}	0.19	0.88	0.29	0.91	−0.22	0.15
K^{+}	0.01	−0.04	0.05	0.84	0.01	−0.29
NO_3^-	0.05	0.13	0.96	0.12	−0.89	−0.15
Cl^-	0.57	0.74	−0.05	0.91	0.02	0.10
SO_4^{2-}	0.70	0.35	0.30	0.82	0.01	0.05
F^-	−0.42	0.40	−0.27	0.12	−0.20	−0.70
Eigen values	5.08	2.16	1.18	5.83	1.95	1.44
% variance	46.23	19.64	10.78	53.03	17.81	13.17

NOTE: TDS = Total Dissolved Solid; TA = Total Alkalinity; TH = Total Hardness.

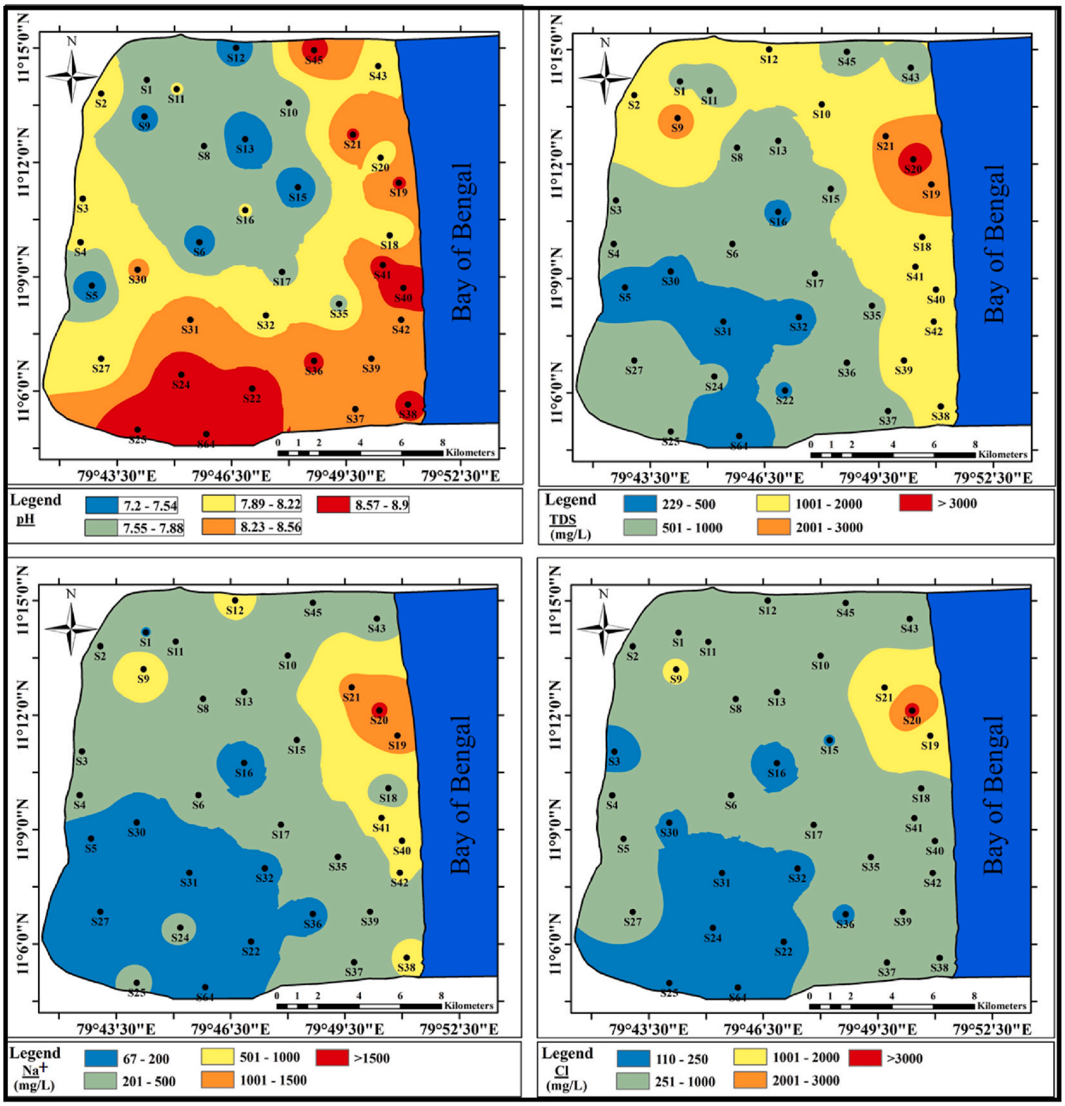

Fig. 3. Spatial distribution of pH, TDS, Na^+ and Cl^- in Cauvery and Uppanar River Basin.

TDS. Cations like Ca^{2+} ranged from 12 to 92 mg/l, and 32 to 356 mg/l; Mg^{2+} ranged from 36 to 400 mg/l, and 68 to 340 mg/l; Na^+ ranges from 67 to 560 mg/l, and 74 to 1600 mg/l; K^+ ranges from 42 to 280 mg/l, and 63 to 502 mg/l for CRB and URB respectively (Table 1). Similarly, anions viz., Cl^- ranged from 120 to 906 mg/l, and 110 to 3260 mg/l; SO_4^{2-} ranged from 8.80 to 260 mg/l, and 20 to 406.30 mg/l; NO_3^- ranged from 1 to 158.50, and 1 to 328.80 mg/l and its source due to using excessive fertilizers in the area; F^- ranged from 0 to 1.2 mg/l, and 0.10 to 0.70 mg/l, and HCO_3^- ranged from 268.40 to 634.40 mg/l, and 195.20 to 829.60 mg/l, TA ranged from 220 to 520 mg/l, and 160 to 680 mg/l, and TH ranged from 48 to 480 mg/l, and 104 to 560 mg/l for CRB and URB respectively (Table 1). These results strongly imply that the groundwater quality in the coastal area influences sea water intrusion. The spatial distribution of pH, TDS, Na^+ and Cl^- are shown (Fig. 3).

5.2. Hydrochemical facies and its evaluation

Major ion concentrations of groundwater were plotted in the Piper trilinear diagram and Hydrochemical Facies Evolution Diagram (HFE-D) [42,43] to reveal geochemical types of groundwater and understand the seawater intrusion processes (Figs. 4 and 5). Three major water types viz., mixed, fresh and saline types of water represented by Piper diagram. The diagram reveals Ca^{2+}+HCO_3^- fresh type water; Ca^{2+}+Na^++HCO_3^- and Ca^{2+}+Mg^{2+}+Cl^-, mixed type water, and Na^++Cl^- saline type water (Fig. 4). The HFE-D plot has 16 subdivisions, representing the various processes summarized in Table 3. HFE-D represents the main processes going on during the intrusion and freshening phases in the evolution of the hydrochemical facies [44,45]. HFE-D has a better option for representing the hydrochemical processes than using a normal Piper diagram. The Piper plot suggests that more than 50% of the sample of both river

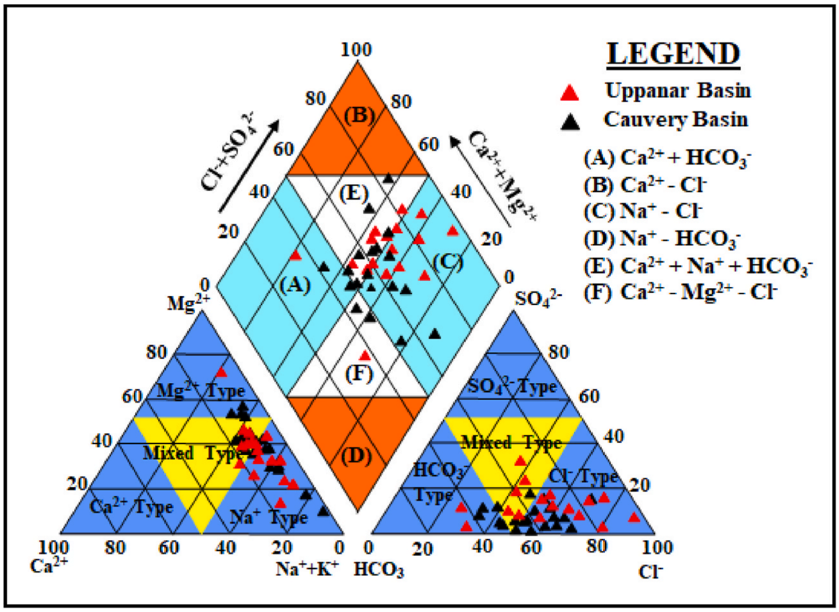

Fig. 4. Piper Plot for the groundwater samples from Cauvery and Uppanar River Basin.

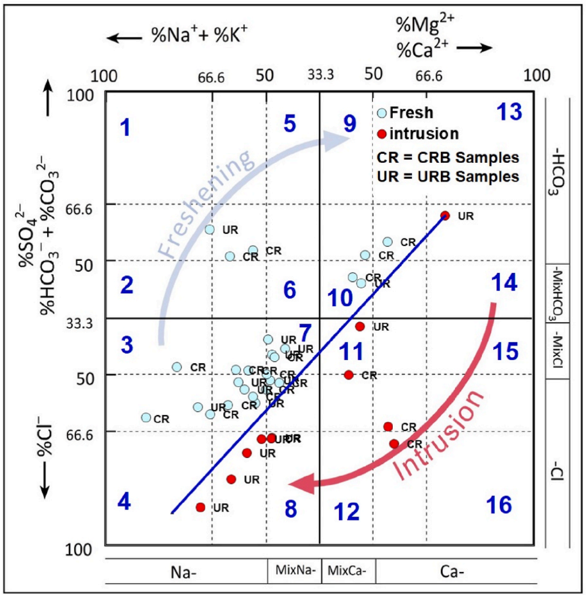

Fig. 5. Hydrochemical Facies Evaluation Diagram (HEF-D) describing the freshwater-saline water mixing processes for Cauvery and Uppanar River Basin.

basins are Na^{+}+Cl^{-} saline water type nature with the domination of strong alkalies (Na^{+}) and strong acid (Cl^{-}) indicating rock-water interaction with the dissolution of minerals by recharging groundwater in aquifer system (Fig. 4). The diagram further suggests that the groundwater was strongly governed by seawater intrusion and salinization, hydrogeochemical and recharge influx processes in the aquifer system [46,47]. The actual recognition of the facies progression classification through recharge and intrusion events was not possible with the Piper diagram [45]. The hydrochemical facies rating diagram (HFE-D) proposed to overcome this difficulty [44]. Groundwater samples from the watershed (CRB and URB) are plotted on the HFE-D plot (Fig. 5). In this plot, seawater (11) and freshwater fields (26) are linked by a mixture line. Four samples Nos. S5, S35, S37, and S39 from CRB, and seven sample Nos. S2, S9, S12, S16, S18, S20, and S21 from URB show saline nature, whereas the remaining samples show the fresh nature of water (Fig. 5). Other divisions denote mixed behaviour of main facies like Na^{+}-MixCl- (Sample Nos. S4, S24, and S38) from CRB, and (Sample No. S15) from URB, Na^{+}-Cl- (Sample Nos. S6, S17, S40, S41, and S42) from CRB, and (Sample Nos. S8, S13, S19, and S45) from URB,

Table 3
Sub-divisions of hydrochemical facies evolution diagram (HFE-D).

Sub-division	Processes/Water facies	No. of Samples in CRB	No. of Samples in URB	Sub-division	Processes/Water facies	No. of Samples in CRB	No. of Samples in URB
1	Na–HCO_3/SO_4	Nil	Nil	9	MixCa-HCO_3/SO_4	Nil	Nil
2	Na-MixHCO_3/ MixSO_4	Nil	1	10	MixCa-MixHCO_3/ MixSO_4	3	1
3	Na-MixCl	2	1	11	MixCa-MixCl	3	Nil
4	Na–Cl	Nil	1	12	MixCa-Cl	1	Nil
5	MixNa-HCO_3/SO_4	2	Nil	13	Ca–HCO_3/SO_4	Nil	Nil
6	MixNa-MixHCO_3/ MixSO_4	Nil	Nil	14	Ca-MixHCO_3/ MixSO_4	Nil	1
7	MixNa-MixCl	8	8	15	Ca-MixCl	Nil	Nil
8	MixNa-Cl	1	4	16	Ca–Cl	Nil	Nil

$MixNa^{+}$-$MixCl^{-}$ (Sample No. S27) from CRB and (Sample Nos. S1 and S11) from URB, Na^{+}-$MixHCO_3^{-}$ (Sample Nos. S25 and S32) from CRB and Sample No. S3 from URB, $MixCa^{2+}$-$MixHCO_3^{-}$ (Sample Nos. S22 and S36) from CRB and Sample No. S10 from URB, and Ca^{2+}-$MixHCO_3^{-}$ (Sample No. S64) from CRB (Fig. 5). The complications of salinization and associated hydrogeochemical processes are clear from this diagram.

5.3. Bivariate plots

Hydrogeochemical processes and groundwater evolution can be better understood through cross-diagrams of various ions. The plots of TDS *vs.* Cl^{-} ions and Na^{+} *vs.* Cl^{-} are generally used for the detection of saline water intrusion [30]. The cross plots of TDS *vs.* Cl^{-} ($R^2 = 0.79$) and Na^{+} *vs.* Cl^{-} ($R^2 = 0.61$) for CRB show a strong and good positive correlation (Fig. 6a and b). Similarly, cross plots of TDS *vs.* Cl^{-} ($R^2 = 0.83$) and Na^{+} *vs.* Cl^{-} ($R^2 = 0.88$) for URB show a strong positive correlation (Fig. 6a and b) indicating more possible seawater intrusion. The increased salinization content is a combined effect of groundwater admixture with seawater and rock-water interaction processes [48]. The high correlation factor of these plots for URB rather than CRB advises most of the groundwater samples were derived from the seawater intrusion in URB with a common source of their origin. The ratio of Na^{+} *vs.* Cl^{-} for CRB ranges from 0.20 to 1.75 with an average value of 0.80 and for URB it ranges from 0.40 to 2.09 with an average value of 0.87. The mean Na^{+} *vs.* Cl^{-} (0.87) molar ratios for the URB were very similar to the assumed seawater ratio (0.86) [49]. The occurrence of Na^{+} and Cl^{-} ions has high values in the groundwater regime due to the dissolution of halite minerals and the combined effect of rock-water interaction and ion exchange reaction in the aquifer [50]. The cross plot of Na^{+} *vs.* Cl^{-} for CRB and URB is shown in (Fig. 6b). Elevated concentration of Na^{+} and Cl^{-} ions in the regime of groundwater in a coastal aquifer was due to the mixing of seawater [47]. The other reason for elevated salinity in groundwater is due to the mixing of seawater with fresh water and water-rock-interaction processes that can control the groundwater composition [45]. The cross plots between Ca^{+2} *vs.* Cl^{-} show a weak positive correlation ($R^2 = 0.26$) for CRB and a very good positive correlation ($R^2 = 0.65$) for URB (Fig. 6c) indicating ion exchange processes are more prominent in URB. Likewise, the cross plots between Ca^{+2} *vs.* SO_4^{2-} show a weak positive correlation ($R^2 = 0.35$) for CRB and a good positive correlation ($R^2 = 0.56$) for URB (Fig. 6d) indicating the groundwater quality is mainly controlled by an ion exchange process.

5.4. Classification-based Total Hardness (TH)

Water quality in relation to salinity can be distinguished by plotting TH (mg/l) *vs.* TDS (mg/l) [3]. TH was estimated by totalling the values of Ca^{2+} and Mg^{2+} ions values. The plot for CRB reflects that most of the groundwater samples are hard fresh category and few samples are hard brackish category, while for URB, the plot reflects that few samples are hard fresh category while maximum samples are hard brackish category (Fig. 7). Groundwater samples are observed to be more saline in URB than compared to CRB.

5.5. Water-rock mechanism (Gibbs Plots)

The mechanism of water-rock interaction which controls the groundwater chemistry can be studied by Gibbs plots [51]. Gibbs diagrams can be plotted TDS with $Na^{+}/(Na^{+}+Cl^{-})$ and TDS with $Cl^{-}/(Cl^{-} + HCO_3^{-})$. These plots give useful information on the composition of groundwater and its evolution. These plots expose the rock-dominant type water for the majority of the samples and a few are evaporation-dominant indicating water-rock interaction for CRB and URB (Fig. 8a & b). The predominant factor for hydro-geochemical processes in the aquifer regime controlling water quality will be the chemical alteration of rock-forming minerals in the aquifer regime. The interaction between groundwater and altered materials prevailing in the aquifer, seawater mixing, minerals dissolution, and ion exchange reactions in the shallow aquifer regime governs the composition of groundwater.

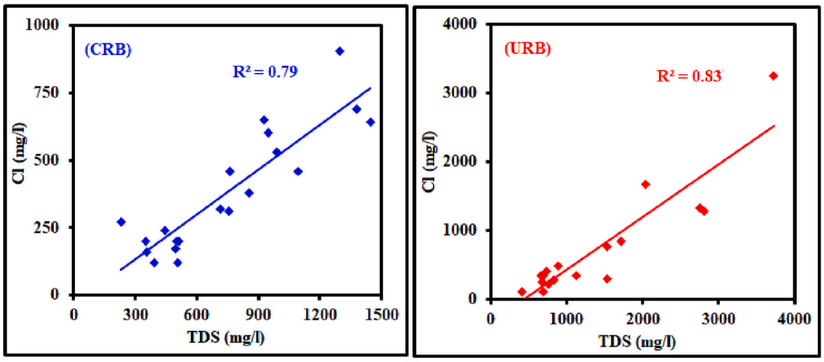

(a)

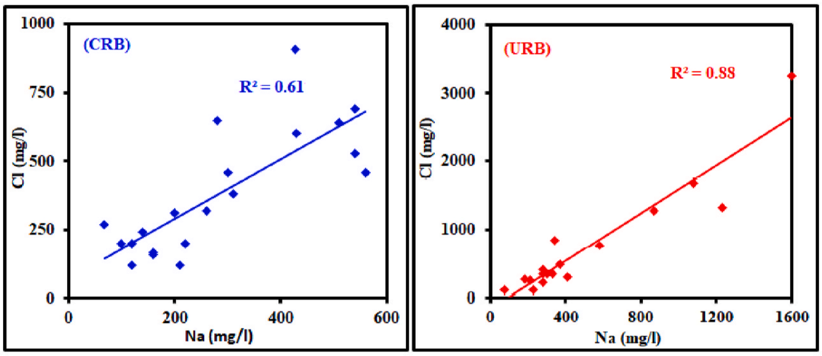

(b)

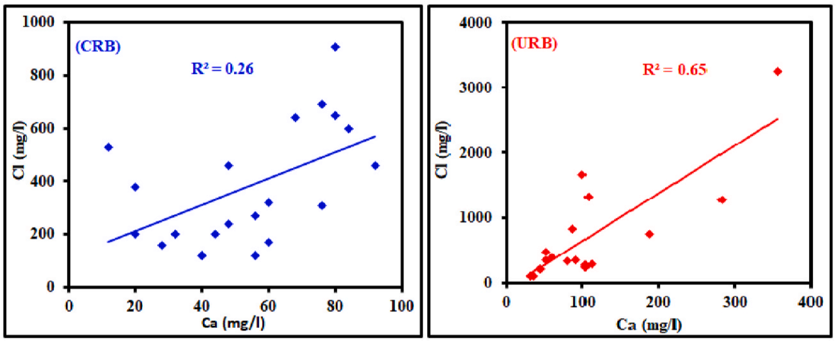

(c)

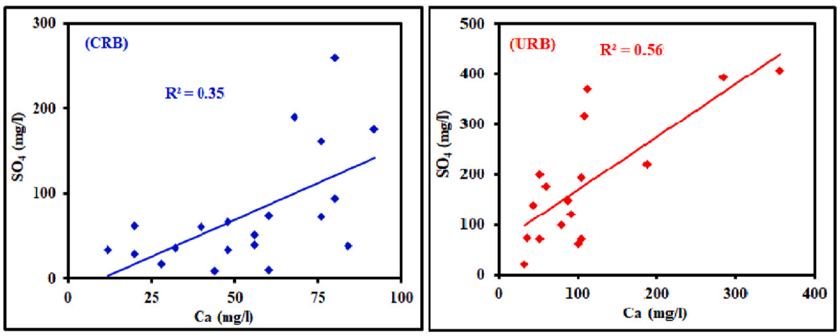

(d)

(caption on next page)

Fig. 6. (a–d): Bivariate plots between different ions (a) TDS vs Cl-; (b) Na vs Cl-; (c) Ca2+ vs Cl- and (d) Ca2+ vs SO4- for Cauvery and Uppanar River Basin.

5.6. *Factor and cluster analyses*

5.6.1. *Factor analyses*

A varimax rotation of the various eigenvalues with factors >1 for URB and CRB is shown in (Table 4). In the URB and CRB, the factors show eigenvalues >1, thus to differentiate the intrusion of seawater a correct interpretation of the factor load.

5.6.2. *Factor analyses in the Cauvery River Basin*

Three factors explain 76.6 % of the total variance, which is enough to provide a good idea of the structure of the data (Table 2). Factor 1 accounted for 46.23 % of the total variance, heavily loaded with TH, Mg^{2+}, Ca^{2+}, and SO_4^{2-}, indicating a salt nature and interaction with rock-water (Table 4). Factor 1 is associated with seawater intrusion in aquifer systems, which increases the concentrations of these ions. The aerial distribution of factor 1 scores for CRB is illustrated (Fig. 9a and Table 4). The figure shows that the area near the shoreline falls over the 0.39 to 2.88 contour line with the S35, S37, and S39 wells. This effect is due to the tsunami, which fills with salty seawater. The second factor explained that 19.64 % of the total variance is strongly related to Na^+, TDS, TA, and Cl^-.

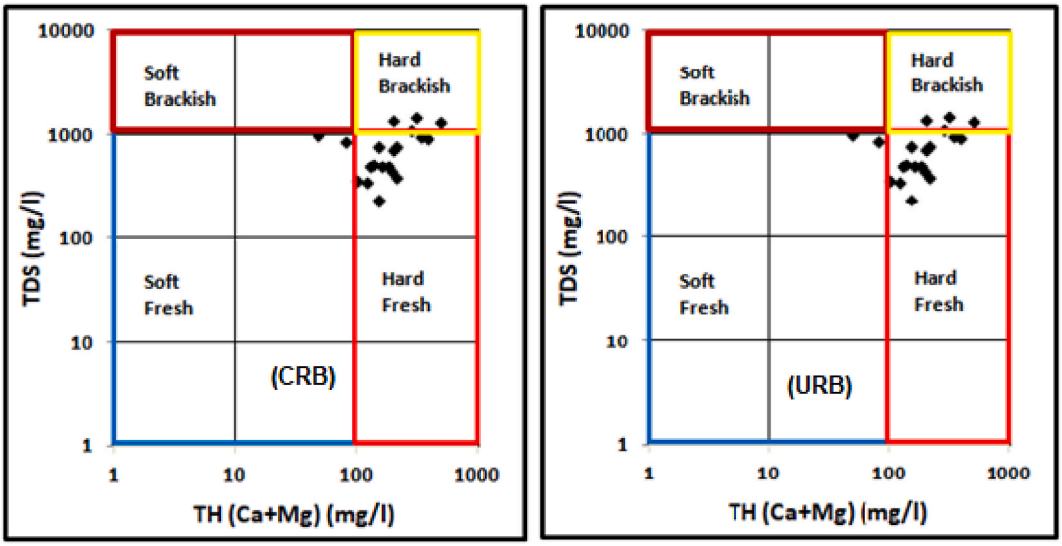

Fig. 7. Classification of groundwater based on TDS and Total Hardness for Cauvery and Uppanar River Basin.

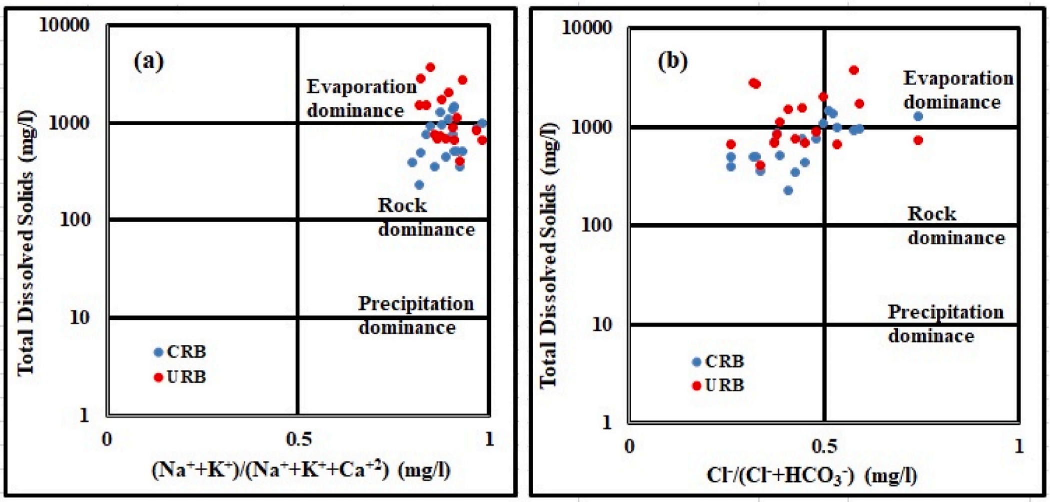

Fig. 8. (a and b): Gibbs plots of the study area showing water-rock interaction (a) Cauvery River Basin and (b) Uppanar River Basin.

Table 4
Factor scores based on groundwater chemistry data of Cauvery River Basin and Uppanar River Basin.

Factor Score	Cauvery River Basin (n = 20)			Uppanar River Basin (n = 17)		
	Factor-1	Factor-2	Factor-3	Factor-1	Factor-2	Factor-3
1	−1.42	1.27	−0.71	−0.70	0.03	−0.35
2	−0.20	−0.94	−0.22	0.13	0.16	1.20
3	−0.26	0.18	−0.41	−0.58	−0.15	−2.09
4	−0.46	0.31	−0.13	−0.28	−0.19	−1.09
5	−0.24	−0.71	0.90	1.47	0.70	0.34
6	−0.62	−0.42	−0.59	−0.63	−0.97	1.05
7	−0.32	−0.68	−0.15	−0.38	0.72	−0.24
8	0.41	−0.54	1.26	0.11	0.69	1.05
9	0.28	−1.15	−0.42	−0.50	0.73	−0.64
10	−0.43	−1.20	−0.11	−0.69	0.25	0.09
11	−0.60	−1.05	−0.22	−0.99	0.11	−0.32
12	1.05	0.18	−0.34	−0.04	0.10	−0.01
13	−0.59	−0.63	−0.46	1.20	−3.30	−0.65
14	1.57	−0.00	−0.69	2.89	1.18	−0.71
15	0.51	0.41	3.64	0.13	−0.60	2.20
16	2.60	0.66	−0.66	−0.41	0.13	0.29
17	−1.92	1.70	0.23	−0.73	0.36	−0.11
18	−0.04	1.71	0.14			
19	0.75	1.80	−0.71			
20	−0.04	−0.89	−0.30			

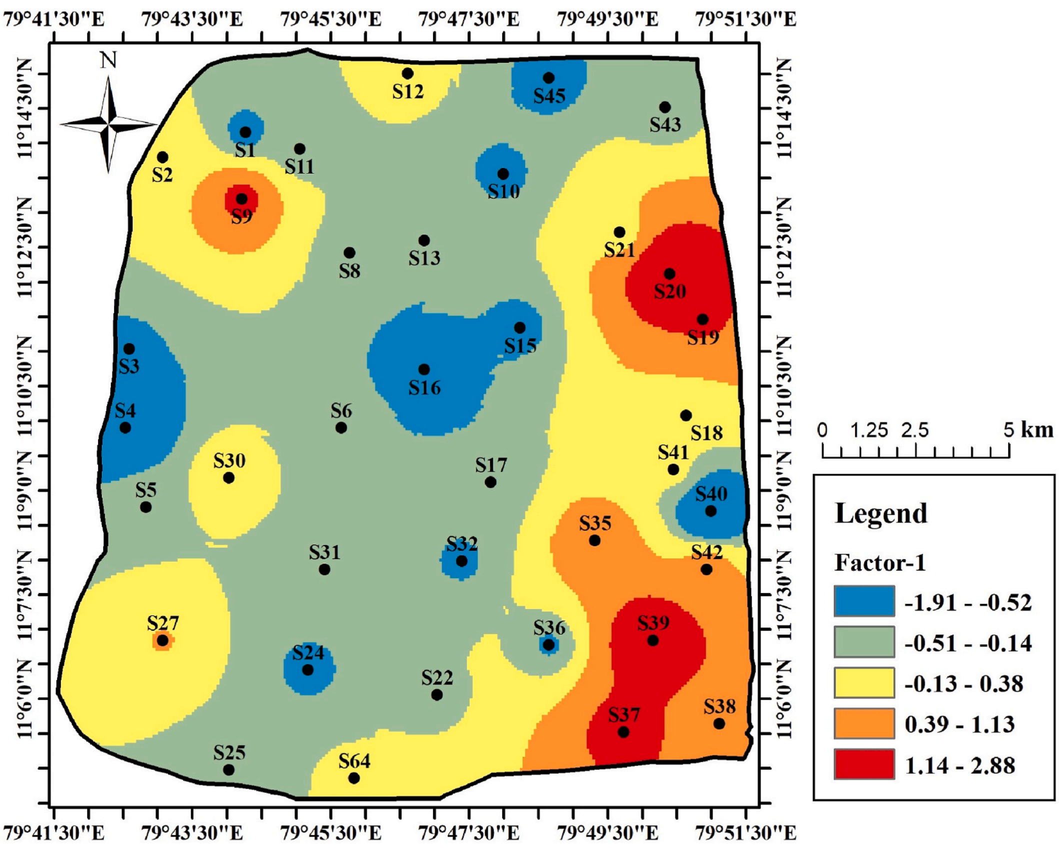

Fig. 9a. Factor 1 contour patterns for Cauvery and Uppanar River Basin.

Thus, the second factor suggests their contribution from saline sources. The aerial distribution of factor scores for Factor-2 of CRB (Fig. 9b and Table 4). From the figure, the area near the coastal line falls above the 0.19 to 1.8 contour line with well Nos. S38, S39, S40, S41, and S42 due to the Tsunami effect, which turns the saline water. For Factors-3, the strong positive loading is for NO_3^-. Further, the NO_3^- has no significant lithologic source in the area and is mainly associated with the surface run-off of nitrate fertilizer

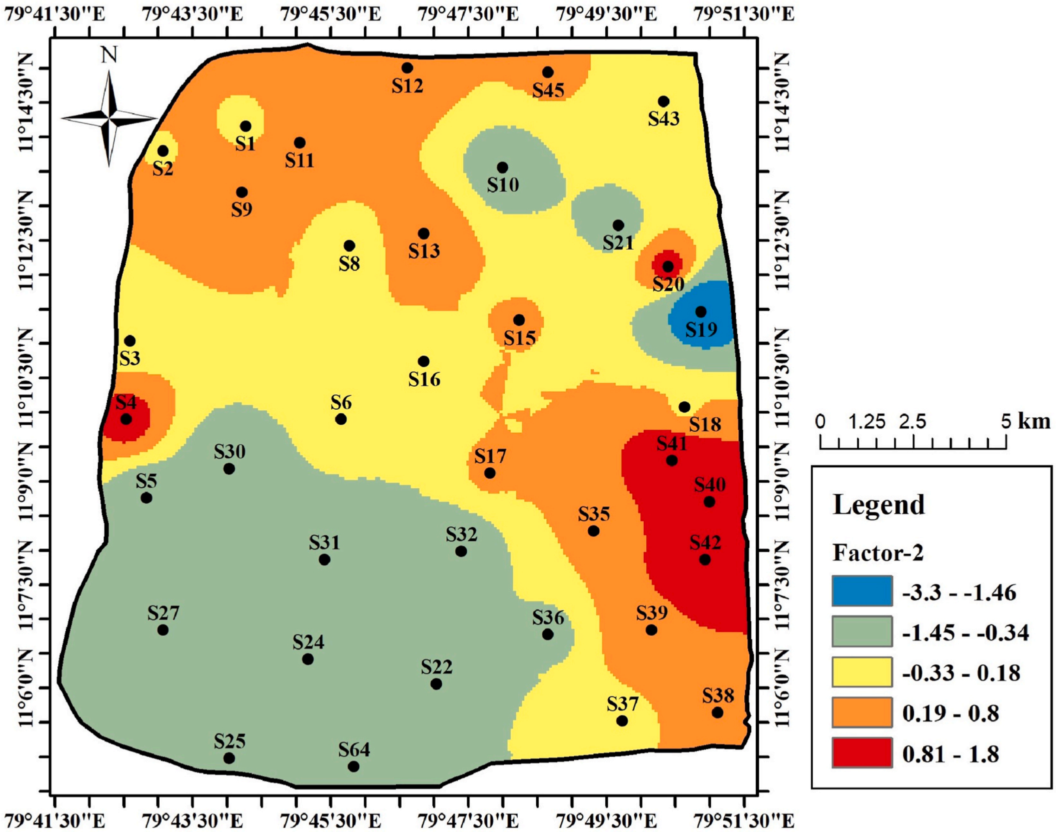

Fig. 9b. Factor 2 contour patterns for Cauvery and Uppanar River Basin.

used for agricultural purposes and also due to anthropogenic sources. Fig. 9c shows the aerial pattern of factor scores for Factor-3 of CRB (Table 4) and observed that the above 1.67 to 3.64 contour lines near to the coastal line with well No. S39.

5.6.3. Factor analyses in the Uppanar River Basin

Three factors explain 84.02 % of the total variance in URB, which is adequate to give a better-quality suggestion of data structure (Table 2). Factor-1 amounts for 53.03 % of the variance, with strong positive loading with TDS, Na^+, Cl^-, Ca^{2+}, K^+, SO_4^{2-}, and TH, indicating the water's saline nature (Table 2). Most of these elements are likely to be common origin from seawater. TDS, Na^+, Cl^-, Ca^{2+}, and K^+ concentrations in seawater are much greater than that in inland water. Factor-1 can be associated with the intrusion of seawater into the aquifer system, with elevated concentrations of these ions. Fig. 9a shows the areal pattern of Factor-1 score for URB (Table 4). From the figure it is observed that the area near the coastline i.e. at well Nos. S19, S20, S21, and towards the inland, a pocket at S9 falls above the 0.39 to 2.88 contour line. This is mainly due to the Tsunami effect, aquaculture activities carried out at the S9 pocket, over drafting of the groundwater in the area and backwaters are the main factors for the migration of seawater which in turn is filled by the saline seawater. Factor-2 explained that 17.81 % of the total variance was found to be weakly associated with the Ca^{2+} and with strong negative loading of TA, and NO_3^-. Fig. 9b shows the areal pattern of factor scores for Factor-2 of URB (Table 4). It is observed from the figure that the area towards inland i.e. at well Nos. S9, S11, S12, S13, S15, and S45, towards the coast, and a pocket at S21 fall above the −0.34 to −3.3 contour line. This is mainly due to the extensive agriculture activity carried out and at S21 pocket is Tsunami effect and by aquaculture activities. Factor-3 explained 13.17 % of the total variance and is strongly associated with the Mg^{2+} and with strong negative loading of Fluoride ion, indicating the interaction of water with the lithological formation was high. High concentrations of Mg^{2+}, with an average of 198 mg/l (Table 1), are observed in the area. This may be due to the uptake of Mg^{2+} by ion exchange sites on clay and other magnesium-bearing minerals [46]. Fig. 9c shows the areal pattern of factor scores for Factor-3 of URB (Table 4). It is observed from the figure that the area towards inland i.e. at well Nos. S3, S4, S8, S13, S19, and S20, towards the coast a pocket at S21 falls below the 0.01 to −2.09 contour line. This is mainly due to the extensive agriculture activity carried out and at S21 pocket is Tsunami effect and aquaculture activities.

5.6.4. Cluster analysis

Through cluster analyses using Ward's method, the relationship between the stations and Euclidean distance similarity measures, and synthesized in dendrograms were obtained for CRB and URB. The variables used as TDS, Na^+, Cl^-, TA, TH, Ca^{2+}, Mg^{2+}, K^+, SO_4^{2-},

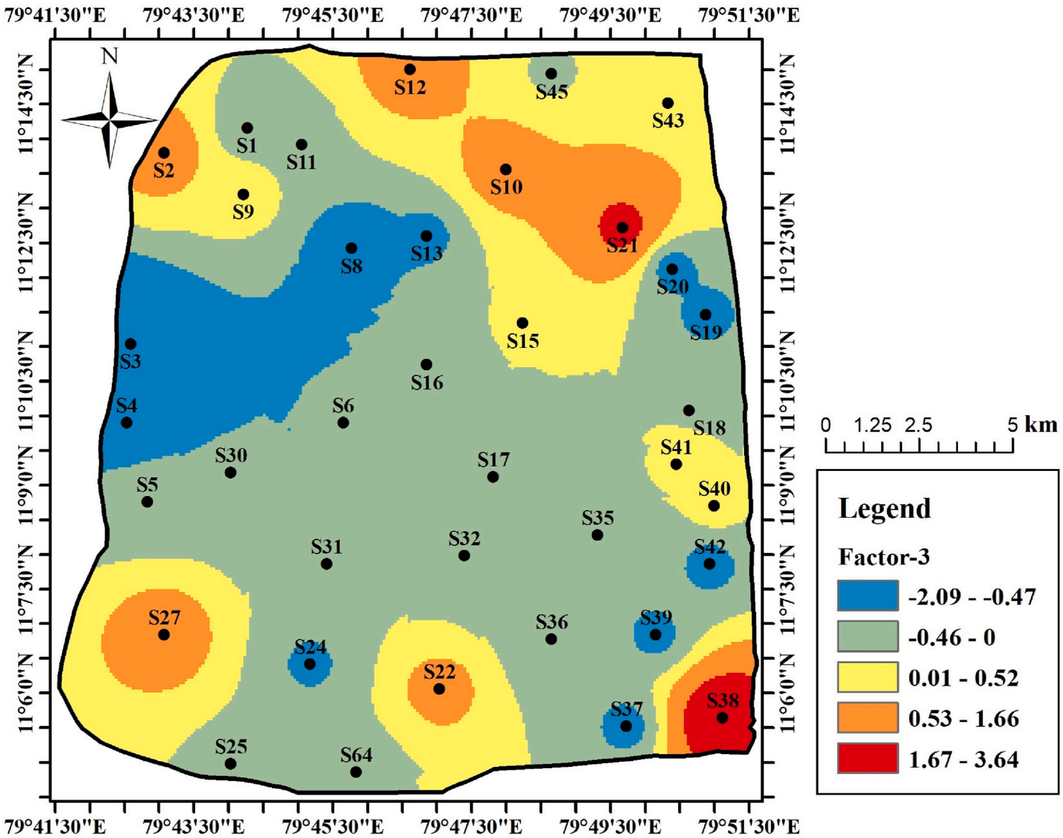

Fig. 9c. Factor 3 contour patterns for Cauvery and Uppanar River Basin.

NO_3^-, and F^-. The performance of dendrograms was done separately for both basins for a better assessment concerning the level of salinity and associated sequences. The CA is performed on the factor score of each sampling point to the factors to illustrate how clusters are distributed, and the cluster results in two basins are shown in (Figs. 10 and 12). The dendrograms indicate the factor score associated with the sample numbers and are categorized into different groups (Figs. 11 and 13).

5.6.5. Cluster analyses for Cauvery River Basin

In CRB, CA is rendered as dendrograms (Fig. 11), where all the 20 sampling points were considered and categorized into six statistically significant groups as in (Table 5a). Five major groups of sites were substantially generated by the clustering procedure, as the ionic characteristics features in this group have some similarities. In group-1 as mentioned in (Table 5a), constitutes seven samples, sample S37 is close to the coastline showing an increase in Cl^- concentration, and samples S35 and S17 are inland but close to a stream showing an increase in Cl^- and Na^+ concentration and other four samples shows their chemical characteristics well within the

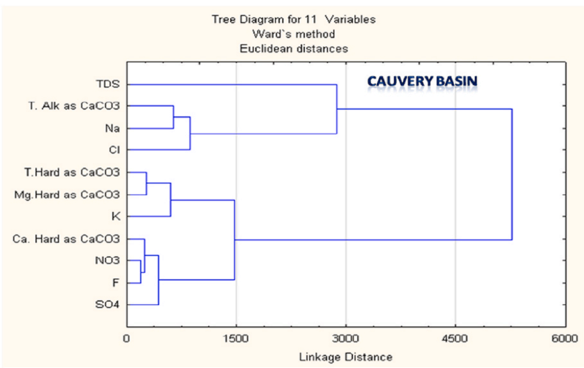

Fig. 10. Cluster Analysis with chemical ions of Cauvery River Basin.

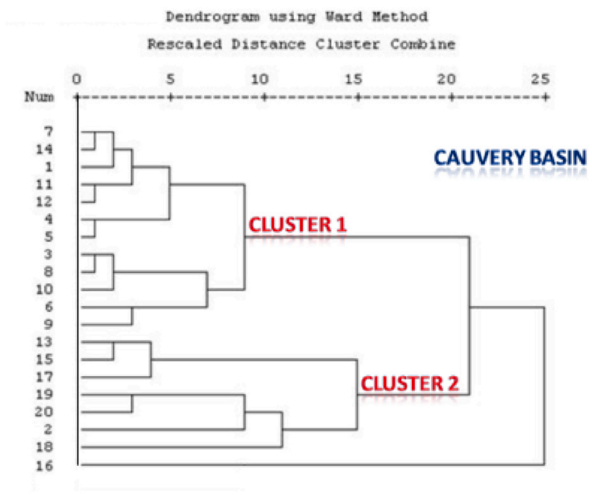

Fig. 11. Cluster analysis with factor score of cauvery river basin.

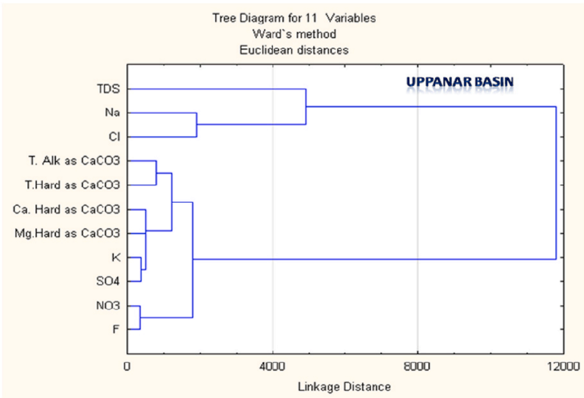

Fig. 12. Cluster analysis with chemical ions of Uppanar River Basin.

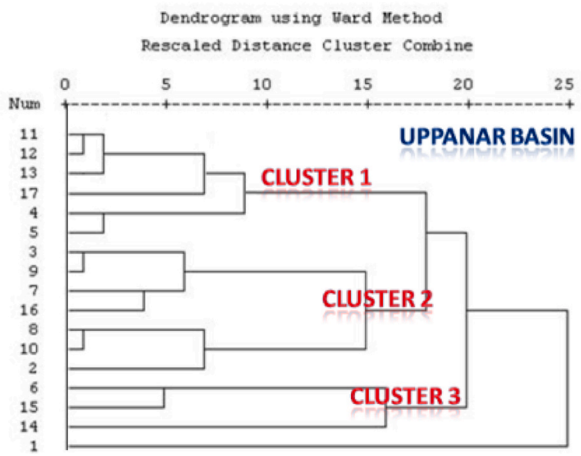

Fig. 13. Cluster analysis with factor score of uppanar river basin.

Table 5a
Samples of cauvery river basin with numbers of dendrogram.

Groups	Samples of Cauvery river basin with numbers of dendrogram
1	S25 (7), S37 (14), S4 (1), S32 (11), S35 (12), S17 (4), S22 (5)
2	S6 (3), S27 (8), S31 (10), S24 (6), S30 (9)
3	S36 (13), S38 (15), S40 (17)
4	S42 (19), S64 (20), S5 (2)
5	S41 (18)
6	S39 (16)

permissible limits indicating a fresh in nature. In group-2 as mentioned in (Table 5a) constitutes five samples in which sample S27 is inland but close to a stream showing an increase in Cl^- concentration and the other four samples show their chemical characteristics well within the permissible limits indicating a fresh in nature. In group-3 and group-4 as mentioned in (Table 5a), each group constitutes three samples where the samples S38, S40, and S42 are close to the coastline showing an increase in TDS, Na^+, and Cl^- concentration, and sample S5 is inland but close to a stream showing an increase in Cl^- concentration, and other two samples show their chemical characteristics are well within the limits indicating a fresh in nature. In groups 5 and 6 as mentioned in (Table 5a), each group constitutes one sample where in both samples S39 and S41 are close to the coastline showing an increase in TDS, Na^+, and Cl^- concentration with samples showing their chemical characteristics like saline in nature.

5.6.6. Cluster analyses for Uppanar River Basin

In URB, CA is rendered as dendrograms (Fig. 13), where all 17 sampling points were considered and categorized into five statistically significant groups as in (Table 5b). Five major groups of sites were substantially generated by the clustering procedure, as the ionic characteristics features in this group have some similarities. In group 1 as mentioned in (Table 5b), it constitutes six samples where in which the samples S18 and S19 are close to the coastline and other samples S16, S45, S8, and S9 are inland but all six samples show their chemical characteristics like TDS, Na^+, and Cl^- very high and indicating the saline nature.

Group 2 as mentioned in (Table 5b), constitutes four samples where sample S43 is close to the coastline and other samples S3, S13, and S11 are inland but all four samples show their chemical characteristics like Na^+, and Cl^- very high indicating the saline nature. In groups 3 and 4 as mentioned in (Table 5b), each group constitutes three samples where the samples S20 and S21 are close to the coastline, and other samples S12, S15, S2, and S10 are inland but all three samples in each group show their chemical characters like TDS, Na^+, and Cl^- very high indicating the saline nature.

Group 5 as mentioned in (Table 5b) constitutes one sample, sample S1 is inland but this sample also has its chemical characteristics like Cl^- very high and indicating the saline nature. The above-mentioned values like TDS, Na^+, and Cl^- are high near the coast due to the Tsunami effect and in the case of inland samples, it is due to huge agriculture and aquaculture activities and a long-time backwater effect.

6. Conclusions

The groundwater quality data from CRB and URB was analyzed for major ions chemistry. TDS concentration ranges from 229 to 1446 mg/l and 408 to3732 mg/l; Na^+ concentration ranges from 67 to 560 mg/l and 74 to1600 mg/l and Cl^- concentration ranges from 120 to 906 mg/l and 110 to3260 mg/l for CRB and URB respectively. A bivariate plot for different ions indicates that the seawater intrusion processes occur in the area with the dissolution of minerals, rock-water interaction, and ion exchange reaction in the groundwater aquifer. The intrusion is more in URB than in CRB. Factor analyses study confirm and are useful in interpreting the hydrochemistry data into a meaningful decision in identifying the seawater intrusion processes. Three factors explain 84.02 % of the total variance in URB. Factor-1 amounts for 53.03 % with strong and positive loading of TDS, Na^+, Cl^-, Ca^{2+}, K^+, SO_4^{2-} and TH, which indicates the saline nature of the water due to over-extractions, high tides, and aquaculture activities. The third factor amounts to 13.17 % of the total variance and is strongly related to the magnesium hardness and with strong negative loading of Fluoride. This factor loading indicates that the water-rock interaction is high due to the uptake of Mg^{2+} by ion exchange sites on clay and other magnesium-bearing minerals. Three factors amount to 76.6 % of the total variance in CRB. Factor 1 amounts to 46.23 % of the total variance, which is strong positive loading with TH, Mg^{2+}, Ca^{2+}, and SO_4^{2-} which indicates saline nature and rock-water interaction. Factor 2 amounts to 19.64 % of the total variance and is found to be strongly associated with Na^+, TDS, Total Alkalinity, and Cl^-, and suggests the contribution was saline sources. Factor 3 the strong positive loading for NO_3^- indicates anthropogenic sources. The CA is

Table 5b
Samples of uppanar river basin with numbers of dendrogram.

Groups	Samples of Uppanar river basin with numbers of dendrogram
1	S16 (11), S18 (12), S19 (13), S45 (17), S8 (4), S9 (5)
2	S3 (3), S13 (9), S11 (7), S43 (16)
3	S12 (8), S15 (10), S2 (2)
4	S10 (6), S21 (15), S20 (14)
5	S1 (1)

performed and the factor score of each sampling point to the factors to illustrate how clusters are distributed and the results of the clustering of ions were observed. In URB the TDS, Na^+, and Cl^- ions make a cluster with a linkage distance of 5000 m and the remaining ions are at a distance of 1800 m. whereas in CRB the TDS, Na^+, Cl^-, and Total Alkalinity ions make a cluster with a linkage distance of 2800 m and the remaining ions are at a distance of 1500 m. The entire analysis gives a conclusion that the streams are acting as one of the sources of the saline water intrusion in URB and CRB, but this intrusion is high in URB due to over-extractions, high tides, and aquaculture activities.

Data availability statement

No data was used for the research described in the article.

Funding

The author declares that no funds or grants are available.

CRediT authorship contribution statement

Ratnakar Dhakate: Writing – review & editing, Writing – original draft, Supervision, Formal analysis, Conceptualization.

Declaration of competing interest

The authors declare that they have no known competing financial interests or personal relationships that could have appeared to influence the work reported in this paper.

Acknowledgment

The author is grateful to the Director, CSIR-National Geophysical Research Institute, Hyderabad, for his kind permission to publish this article. Authors express their sincere thanks to the Editor-in-Chief for his encouragement and support. The author also thanks the anonymous reviewers for their constructive and scientific suggestions for improving the manuscript standard. The manuscript Reference No. is NGRI/Lib/2023/Pub-94.

References

[1] N. Subba Rao, I.S. Nirmala, K. Suryanarayana, Groundwater quality in a coastal area: a case study from Andhra Pradesh, India, Environ. Geol. 48 (2005) 543–550, https://doi.org/10.1007/s00254-005-1306-2.
[2] K. Kantamaneni, X. Du, S. Aher, R.M. Singh, R, Building blocks: a quantitative approach for evaluating coastal vulnerability, Water 9 (2017) 905, https://doi.org/10.3390/w9120905.
[3] Dhakate Ratnakar, G. Venkata Ratnalu, S. Sankaran, Hydrogeochemical and isotopic study for assessment of saline water ingression into shallow coastal aquifers of Udupi District, Karnataka, India, Geochem. J. 80 (4) (2020). Article No. 125647.
[4] M. van Camp, Y. Mtoni, I.C. Mjemah, C. Bakundukize, K. Walraevens, Investigating sea-water intrusion due to groundwater pumping with schematic model simulations: the example of the Dar es Salaam coastal aquifer in Tanzania, J. Afr. Earth Sci. 96 (2014) 71–78.
[5] P.M. Barlow, E.G. Reichard, Saltwater intrusion in coastal regions of North America, Hydrogeol. J. 18 (2010) 247–260, https://doi.org/10.1007/s10040-009-0514-3.
[6] K.A. Allow, Seawater intrusion in Syrian coastal aquifers, past, present and future, case study, Arabian J. Geosci. 4 (2011) 645–653, https://doi.org/10.1007/s12517-010-0261-8.
[7] G. Felisa, V. Ciriello, V. Di Federico, Saltwater intrusion in coastal aquifers: a primary case study along the Adriatic Coast investigated within a probabilistic framework, Water 5 (2013) 1830–1847, https://doi.org/10.3390/w5041830.
[8] C. Garing, L. Luquot, P.A. Pezard, P. Gouze, Geochemical investigations of saltwater intrusion into the coastal carbonate aquifer of Mallorca, Spain, Appl. Geochem. 39 (2013) 1–10, https://doi.org/10.1016/j.apgeochem.2013.09.011.
[9] L. Shi, J.J. Jiao, Seawater intrusion and coastal aquifer management in China: a review, Environ. Earth Sci. 72 (2014) 2811–2819, https://doi.org/10.1007/s12665-014-3186-9.
[10] E. Suhartono, P. Purwanto, S. Suripin, Seawater intrusion modeling on groundwater confined aquifer in Semarang, Procedia Environ. Sci. 23 (2015) 110–115, https://doi.org/10.1016/j.proenv.2015.01.017.
[11] F. Abdalla, Ionic ratios as tracers to assess seawater intrusion and to identify salinity sources in Jazan coastal aquifer, Saudi Arabia, Arabian J. Geosci. 9 (40) (2016), https://doi.org/10.1007/s12517-015-2065-3.
[12] S.P. Rajaveni, I.S. Nair, L. Elango, Evaluation of impact of climate change on seawater intrusion in a coastal aquifer by finite element modelling, J. Clim. Change 2 (2016) 111–118, https://doi.org/10.3233/JCC-160022.
[13] V. Manivannan, L. Elango, Seawater intrusion and submarine groundwater discharge along the Indian coast, Environ. Sci. Pollut. Res. 26 (2019) 31592–31608, https://doi.org/10.1007/s11356-019-06103-z.
[14] G.K. Hodlur, Dhakate Ratnakar, Rolland Andrade, Correlation of vertical electrical sounding and borehole-log data for delineation of saltwater and freshwater aquifers, Geophysics 71 (1) (2006) G11–G20, https://doi.org/10.1190/1.2169847.
[15] G.K. Hodlur, Dhakate Ratnakar, T. Sirisha, D.B. Panaskar, Resolution of freshwater and saline water aquifers by composite geophysical data analysis methods, Hydrol. Sci. J. 55 (3) (2010) 414–434.
[16] Dhakate Ratnakar, V. Satish Kumar, B. Amarender, S. Sankaran, V.V.S. Gurunadha Rao, Integrated geophysical and hydrochemical approach for locating fresh water locations in a coastal terrain, Water Resour. Manag. 29 (9) (2015) 3401–3417.
[17] Dhakate Ratnakar, B. Amarender, V. Satish Kumar, S. Sankaran, V.V.S. Gurunadha Rao, Application of Ground Penetrating Radar for identification of groundwater resources in a coastal terrain, Arabian J. Geosci. 8 (7) (2015) 4703–4715.
[18] Dhakate Ratnakar, S. Sankaran, V. Satish Kumar, B. Amarender, P. Harikumar, S.K. Subramanian, Demarcating saline water intrusion pathways using Remote Sensing, GIS and Geophysical techniques in a structurally controlled coastal aquifers in Southern India, Env, Earth Sci. 75 (5) (2016) 1–19, 363.

[19] V. Satish Kumar, Ratnakar Dhakate, B. Amarnder, S. Sankaran, Application of ERT and GPR for demarcating the saline water intrusion in coastal aquifers of Southern India, Env, Earth Sci. 75 (5) (2016) 1–17. Article No.393.
[20] B. Helena, R. Pardo, M. Vega, E. Barrado, J.M. Fernandez, L. Fernandez, Temporal evolution of groundwater composition in an alluvial (Pisuerga river, Spain) by principal component analysis, Water Res. 34 (2000) 807–816.
[21] R. Raghunath, T.R.S. Murthy, B.R. Raghavan, The utility of multivariate statistical techniques in hydrogeochemical studies: an example from Karnataka, India, Water Res. 36 (2002) 2437–2442.
[22] V. Simeonov, J.A. Stratis, C. Samara, G. Zachariadis, D. Voutsa, A. Anthemidis, M. Sofoniou, T.H. Kouimtzis, Assessment of the surface water quality in Northern Greece, Water Res. 37 (2003) 4119–4124.
[23] V. Simeonov, P. Simeonova, R. Tsitouridou, Chemometric quality assessment of surface waters two case studies, Chemical and Eng, Ecology 11 (6) (2004) 449–469.
[24] P. Simeonova, V. Simeonov, G. Andreev, Analysis of the struma river water quality, Cent. Eur. J. Chem. 2 (2003) 121–126.
[25] K.P. Singh, A. Malik, D. Mohan, S. Sinha, Multivariate statistical techniques for the evaluation of spatial and temporal variations in water quality of Gomti River (India) – a case study, Water Res. 38 (2004) 3980–3992.
[26] M.F. Lanjwani, M.Y. Khuhawar, T.M.J. Khuhawar, M.S. Samtio, S.Q. Memon, Spatial variability and hydrogeochemical characterisation of groundwaters in Larkana of Sindh, Pakistan, Groundwater for Sustainable Development 14 (2021) 100632.
[27] E. Reisenhofer, G. Adami, P. Barbieri, Using chemical and physical parameters to define the quality of karstic fresh waters (Timavo River, North-eastern Italy): a chemometric approach, Water Res. 32 (1998) 1193–1203.
[28] D.A. Wunderlin, M.P. Diaz, M.V. Ame, S.F. Pesce, A.C. Hued, M.A. Bistoni, Pattern recognition techniques for the evaluation of spatial and temporal variations in water quality. A case study: suquia river basin (Cordoba-Argentina), Water Res. 35 (2001) 2881–2894.
[29] J.H. Kim, Hydrogeochemical Study on Shallow Groundwater at the Coastal Area of Kimje, Seoul National University, Seoul, 2001.
[30] J.H. Kim, R.K. Kim, J. Lee, H.W. Chang, Hydrogeochemical characterization of major factors affecting the quality of shallow groundwater in the coastal area at Kimje in South Korea, Environ. Geol. 44 (2003) 478–489.
[31] M.F. Lanjwani, M.Y. Khuhawar, T.M. Jahangir Khuhawar, Assessment of groundwater quality for drinking and irrigation uses in taluka Ratodero, district Larkana, Sindh, Pakistan, Int. J. Environ. Anal. Chem. 102 (16) (2022) 4134–4157.
[32] H. Suk, K.K. Lee, Characterization of a ground water hydrochemical system through multivariate analysis: clustering into groundwater zones, Ground Water 37 (1999) 358–366.
[33] D. Marghade, D.B. Malpe, N. Subba Rao, Applications of geochemical and multivariate statistical approaches for the evaluation of groundwater quality and human health risks in a semi-arid region of eastern Maharashtra, India, Environ. Geochem. Health 43 (2021) 683–703, https://doi.org/10.1007/s10653-019-00478-1.
[34] N. Subba Rao, D. John Devadas, K.V. Srinivasa Rao, Interpretation of groundwater quality using principal component analysis from Anantapur district, Andhra Pradesh, India, Environ. Geosci. 13 (4) (2006) 239–259, https://doi.org/10.1306/eg.02090504043.
[35] M.F. Lanjwani, M.Y. Khuhawar, T.M. Jahangir Khuhawar, A.H. Lanjwani, W.A. Soomro, Evaluation of hydrochemistry of the Dokri groundwater, including historical site Mohenjo-Daro, Sindh, Pakistan, Int. J. Environ. Anal. Chem. 103 (8) (2023) 1892–1916.
[36] J.Y. Lee, J.Y. Cheon, K.K. Lee, S.Y. Lee, M.H. Lee, Statistical evaluation of geochemical parameter distribution in a groundwater system contaminated with petroleum hydrocarbons, J. Environ. Qual. 30 (2001) 1548–1563.
[37] N. Subba Rao, Spatial control of groundwater contamination, using principal component analysis, J. Earth Syst. Sci. 123 (2014) 715–728, https://doi.org/10.1007/s12040-014-0430-3.
[38] M. Ramakrishnan, Tectonic evolution of the Archaean high grade terrain of South India, J. Geol. Soc. India 32 (1988) 118–119.
[39] CGWB (Central Ground Water Board), District groundwater brochure Nagapattinam district, Tamil Nadu, CGWB Technical Report Series, South Eastern Coastal Region, Chennai (2008) 1–15.
[40] APHA (American Public Health Association), Standard Methods for the Examination of Water and Waste Water, APHA, Washington D.C, USA, 1995, 19th edition.
[41] WHO (World Health Organisation), Guidelines to Drinking Water Quality, World Health Organisation, Geneva, 1984, p. 186.
[42] A.M. Piper, A graphical procedure in the chemical interpretation of groundwater analysis, Trans. Am. Geophys. Union 25 (1944) 914–923.
[43] E. Giménez Forcada, F.J. Sánchez San Román, An Excel Macro to Plot the HFE-Diagram to Identify Seawater Intrusion Phases, Groundwater, 2014, https://doi.org/10.1111/gwat.12280 hhttps://org.
[44] E. Gimenez Forcada, Dynamic of seawater interface using hydrochemical facies evolution diagram, Ground Water 48 (2) (2010) 212–216.
[45] G. Ghiglieri, A. Carletti, D. Pittalis, Analysis of salinization processes in the coastal carbonate aquifer of Porto Torres (NW Sardinia, Italy), J. Hydrol. (Wellingt. North) 432–433 (2012) 43–51.
[46] N. Subba Rao, D. Rashmirekha G. Sakram, Understanding the factors contributing to groundwater salinity in the coastal region of Andhra Pradesh, India, Jour, Of Contaminant Hydrology 250 (2022) 104053, https://doi.org/10.1016/j.jconhyd.2022.104053.
[47] S.C. Park, S.T. Yun, G.T. Chae, I.S. Yoo, K.S. Shin, C.H. Heo, S.K. Lee, Regional hydrochemical study on salinization of coastal aquifers, western coastal area of South Korea, J. Hydrol. 313 (2005) 182–194.
[48] A.K. Mohanty, V.V.S. Gurunadha Rao, Hydrogeochemical, seawater intrusion and oxygen isotope studies on a coastal region in the Puri District of Odisha, India, Catena 172 (2019) 558–571, https://doi.org/10.1016/j.catena.2018.09.010.
[49] A. Vengosh, A.J. Spivack, Y. Artzi, A. Ayalon, Geochemical and boron, strontium and oxygen isotopic constraints on the origin of the salinity in groundwater from the Mediterranean coast of Israel, Water Resour. Res. 35 (1999) 1877.
[50] M.S. Andersen, V. Nyvang, R. Jakobsen, D. Postma, Geochemical processes and solute transport at the seawater/freshwater interface of a sandy aquifer, Geochem. Cosmochim. Acta 69 (2005) 3979–3994.
[51] R.J. Gibbs, Mechanisms controlling world water chemistry, Science 170 (1970) 1088–1090.